Spring 2012

# The role of histidines in neurosteroid binding of NMDA GluN2B and D subunits

Sarah Rhoads
*University of Richmond*

# The Role of Histidines in Neurosteroid Binding of NMDA GluN2B and D Subunits

by

Sarah Rhoads

Honors Thesis

in

Program in Biochemistry and Molecular Biology
University of Richmond
Richmond, VA

Date Submitted: April 24, 2012

Advisor: Lisa Gentile

This thesis has been accepted as part of the honors requirements
in the Program in Biochemistry and Molecular Biology.

_____ _____

*(advisor signature)* *(date)*

_____ _____

*(reader signature)* *(date)*

# Table of Contents

Acknowledgements:

I would like to acknowledge first Dr. Lisa Gentile and Krasnodara Cameron for teaching me so much about Biochemistry, proteins, and working in a research lab. Their support has been invaluable. I would also like to thank Laura Zemcik, Shannon Biello, and Sarah Scheurich for their help with the work presented here, as well as the other members of my lab- David Fanelli, Ryan Roark, and Emily Bartle. Thank you to the University of Richmond, especially the ever-amazing Chemistry Department, HHMI, and Beckman for the opportunities I have been given to conduct this research. Finally, I'd like to acknowledge my family and my friends, especially my roommate Carroll, for putting up with me talking about proteins for the last three years.

# I. Abstract

Implicit in cellular mechanisms essential for learning and memory, NMDA receptors are heterotetrameric members of the family of ionotropic glutamate receptors. Activation of the glutamate-specific receptor subunits results in the opening of ion channels, triggering an excitatory pathway, which can be moderated by certain endogenous and exogenous compounds. Previous research with the endogenous neurosteroids *pregnenolone sulfate* (PS) and *3α-hydroxy-5-β-20-one sulfate* (PregS) have indicated that the binding of these neurosteroids to NMDA receptors containing the four A-D isoforms of the GluN2 subunit affects current flow through them[1]. Binding of PS to NMDA receptors containing GluN2A or GluN2B subunits causes an increased amount of current flow through the channel, whereas binding of PS to receptors containing GluN2C and 2D subunits decreases current flow through these channels. Binding of PregS to any NMDA receptor also decreases current flow. Binding studies from our lab have determined that the neurosteroids PS and PregS bind to the amino terminal domain (ATD) of both GluN2B and GluN2D subunits. The ATD segment used in these studies consisted of residues 121-292. Binding of both neurosteroids was monitored between pH 6.0 and 8.0. Results demonstrated that the binding of PS to GluN2B and D ATDs occurred only between pH 6 and 6.5. PregS showed similar pH dependence for the GluN2B ATD, although binding was restored at pH 8. The pH dependence of neurosteroid binding suggests the importance of a protonated histidine residue in each binding interaction. The GluN2B ATD segment contains one histidine at residue 127, whereas the corresponding GluN2D ATD contains 3 histidines at residues 143, 182, and 202. Results from preliminary structural and neurosteroid binding studies of His to Ala and Gln mutations in the GluN2D ATD are presented.

## II. Background & Introduction

Glutamate is the main excitatory neurotransmitter in the mammalian brain. It is involved in many cognitive functions, including learning and memory formation. Ionotropic glutamate receptors (iGluRs) are a family of ligand-gated ion channels, located in the postsynaptic neural membrane, which open as a response to glycine and the neurotransmitter glutamate and are therefore highly controlled[1]. Glutamate binds to specific receptor subunits via an extracellular binding site, inducing a conformational change that causes a channel to open in the membrane. When the iGluRs are improperly regulated, excess amounts of cations ($Na^{+}$, $Ca^{2+}$, $K^{+}$) enter the postsynaptic neural cell, causing cell death[1]. This misregulation of iGluRs due to over-activity of the receptors has been linked to neurodegenerative diseases such as Huntington's, Alzheimer's, and Parkinson's.

### A. iGluR Family and Structure

Included in the iGluR family are alpha-amino-3-hydroxy-5-methyl-4- isoxazole-propionic acid (AMPA), kainate, delta, and N-methyl-D-aspartate (NMDA) receptors[1]. Each member of the iGluR family is a tetrameric protein, encoded by 18 genes that often undergo RNA editing and alternative splicing[2]. AMPA and kainate receptors are often homotetramers, the NMDA receptor is a heterotetramer. Each subunit from the iGluR family is modular, as shown in Fig. 1, and contains seven domains. They have an amino terminal domain (ATD), which is critical for the interaction between subunits, an extra-cellular S1S2 neurotransmitter (ligand) binding domain (LBD), three membrane-

spanning domains, a re-entrant loop, which forms the pore when the receptor is assembled, and a C-terminal tail that is intracellular[1].

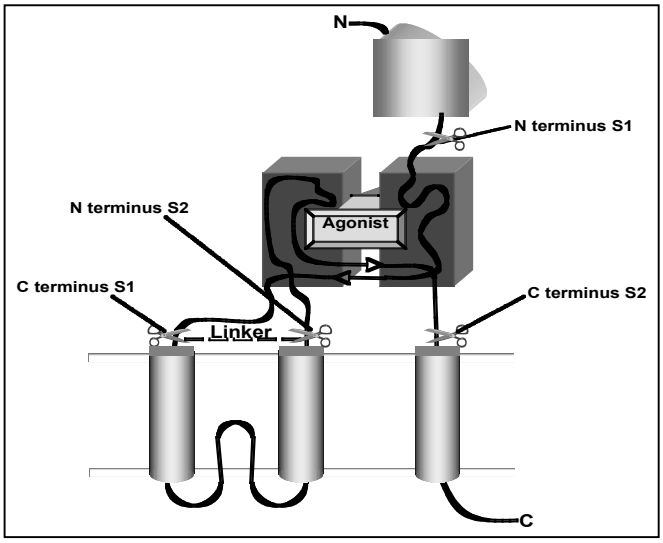


*Fig 1:* Schematic representation of GluR2 domain architecture, composed of extracellular amino terminal domain, S1S2 ligand-binding domain (LBD), three transmembrane-spanning regions, a re-entrant loop, and an intracellular carboxyl terminal tail.

The NMDA heterotetramer is composed of two GluN1 subunits, which are one of eight alternatively spliced versions from a single gene, and two GluN2 subunits (Fig. 2), which are one of four versions from separate genes[2]. The GluN2 subunits are named as GluN2A-D. As shown in Fig. 2, GluN1 subunits bind glycine, while GluN2 subunits bind the neurotransmitter glutamate. Glutamate binds to the GluN2 subunit as an agonist, and glycine binds to the GluN1 subunit as a coagonist.

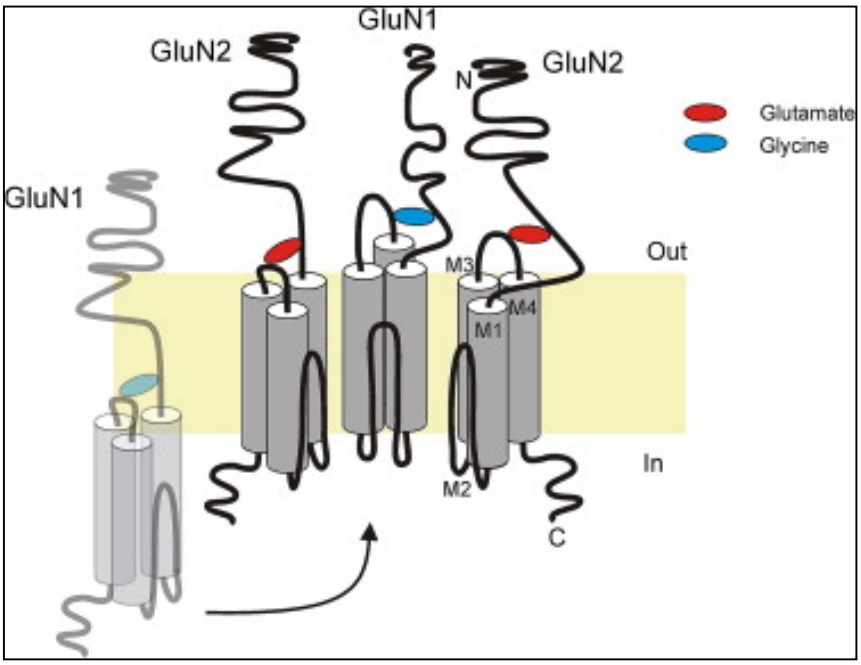


*Fig 2*: The schematic representation of NMDA receptor. NMDA receptor consists of four subunits with the ion channel pore in the center. Each subunit is composed of an intracellular C-terminus, four membrane domains (M1–4) and extracellular region, where glycine or glutamate binds[3].

The iGluR family is divided according to sequence homology and agonist specificity, creating functional heterogeneity that is important for the complex functioning of glutamatergic neuro-transmission[4]. While both receptors are found on the extrasynaptic plasma membranes, AMPA receptors are intracellularly associated with the endoplasmic reticulum, golgi apparatus, and multi-vesicular bodies[4]. In contrast, the majority of NMDA receptors are expressed on the surface of neurons, concentrated around synaptic junctions[4].

### 1. The Amino Terminal Domain

While there is much still left to learn about the ATD, recent years have greatly elucidated its structure and function. Studies done on NMDA receptor assembly indicate

that GluN1 and GluN2 amino terminal domains likely heterodimerize and subsequently associate[5]. This association of two heterodimers is believed to play a key role in determining correct NMDA receptor subunit assembly. The ATD was successfully proven to control the kinetics of NMDA receptor deactivation. It was also determined that the ATD- ligand binding domain linker has an important role in generating this effect, and that transplantation of the ATD affected the gating properties of the NMDA receptor subtypes concerned.

**2. The S1S2 Ligand Binding Domain**

Although there is currently only one crystal structure for a full-length iGluR, crystal structures have been found for the isolated LBDs in 10 subunits of both NMDA and AMPA receptors. In AMPA receptors, it has been shown that the LBD is the site of action of positive allosteric modulators, some of which cause desensitization while others slow excitatory current decay, and recent crystal structures of these GluA2 modulator complexes have been solved[6]. The ligand binding domain consists of two lobes that close together upon agonist binding, forming a clamshell-like structure[7]. In addition to the elucidation of these crystal structures, free energy landscape measurements of the GluA2 LBD in apo and glutamate bound states shows multiple conformations of similar energy for the apo protein, which is consistent with the growing idea of a highly dynamic molecule[8]. Simulations have been used for studying the spontaneous opening and closing of GluA2, GluK, and NMDA GluN2A subunit LBDs as well, which demonstrate a salt bridge network surrounding the clamshell that likely acts as a ligand binding sensor to trigger domain closure[9].

### 3. Full Length iGluR

The crystal structure of a full-length rat GluA2 AMPA receptor tetramer has recently been determined using X-ray data to 3.6 Å resolution. While this resolution is not enough to elucidate specific side chains, it is the first full-length crystal structure of an iGluR tetramer to be found[10]. The crystal structure showed several interesting aspects of the GluA2 structure, particularly a cross-over of subunits that form dimer pairs in the layers of the amino terminal (ATD) and ligand binding (LBD) domains[10] (Fig. 3). It appears that the ATD and LBD tetramer assemblies are loosely packed, as evidenced by a large cavity observed on the central axis of symmetry at the ATD and LBD interface[10].

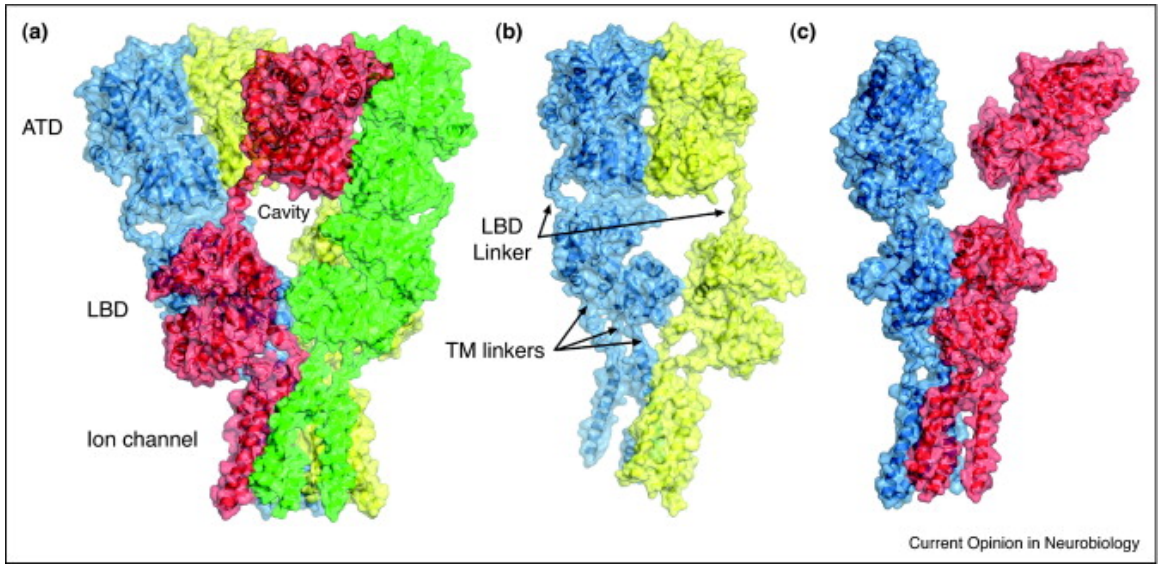


*Fig 3:* Domain organization in the GluA2 ion channel crystal structure (PDB 3KG2). **(a)** The four subunits in the tetramer assembly are colored blue, yellow, red and green; the molecular surface representation reveals key features of the structure, including its organization in layers, the cavity at the ATD and LBD interface, and the large size of the extracellular domains compared to the ion channel. **(b)** ATD dimer formed by chains A and B reveals a large separation of the LBD domains in this subunit pair; linkers that connect the layered domains are indicated by black arrows that draw attention to the different conformations of the LBD linkers in the A and B subunits. **(c)** LBD dimer formed by chains A and D reveals a large separation of the ATD domains in this subunit pair[11].

Additional studies on wild type GluA2 receptors revealed that AMPA receptor assembly proceeds starting with the formation of dimers, during which the ATD couples closely with the trans-membrane segments, whereas the ligand binding domains (LBDs) wind up pushed to the side. For AMPA receptors, subunit exchange in the ATD and LBD layers appears to be critical to tetramer assembly[12].

## B. PS & PREGAS

Several endogenous compounds, such as Zn (II), the polyamines spermine and spermidine, and the sulfated neurosteroids pregnenolone sulfate (PS) and 3-α -hydroxy-5-β-pregnan-20-one sulfate (PregS) have been shown to be involved in the regulation of the iGluRs[13]. PregS is a representative member of neurosteroids that, as shown in Fig. 2, inhibit the activity of NMDA receptors, as well as $GABA_A$, AMPA, and kainate receptors[13]. These neurosteroids have been shown to reduce open channel probability and time, as well as increase receptor desensitization[14]. PregS has been demonstrated to be an allosteric inhibitor of NMDA receptors, rather than an ion channel blocker or competitive inhibitor with glutamate[15]. Studies have indicated that a PregS inhibitory binding site is likely located on the GluN2 subunit, although the exact location is uncertain[16]. It is the elucidation of this neurosteroid binding site that is the focus of this work.

PS, which is structurally similar to PregS except for one double bond at the steroid A/B ring juncture and different orientations of the sulfate group that both neurosteroids possess- β orientation in PS, and α orientation in PregS (Fig. 4), inhibits

the activity of non-NMDA iGluRs but differentially regulates NMDA receptors[17]. Potentiation with PS has been shown to induce a 200% rise in NMDA receptor response, and is believed to be exerted allosterically, via binding to a potentiating site on the receptor[3]. Studies have demonstrated that PS has dual inhibitory and potentiating activity at NMDA receptors with GluN2A or B subunits, with potentiation prevailing in 2A or B subunits but inhibition prevailing in NMDA receptors with GluN2C or D subunits[18]. In studying PS potentiation it was found that the potentiating effect of the neurosteroid was significantly stronger when PS was bound to the receptor prior to the agonist, nearly 400% compared to 80% potentiation when PS was simultaneously bound with glutamate[19]. This indicates that the PS binding site might interact allosterically with the glutamate binding site, although again the exact binding site of both neurosteroids in question, PS and PregS, has yet to be elucidated.

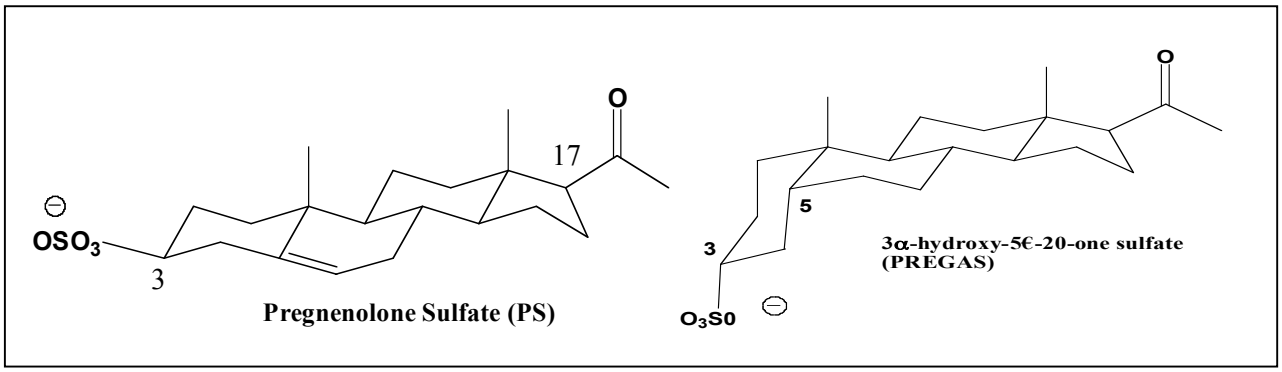


*Fig 4:* Neurosteroid structures of PS and PregS

One of the primary structural similarities of PS and PregS, shared with all steroids that are capable of modulating NMDA receptor function, is the presence of a charged group on the C3 of the steroid core, in the case of PS and PregS a sulfate group (Fig 4)[20]. It has also been shown that more planar steroids, of which PS is a characteristic member

due to its double bond, typically function as potentiators of NMDA receptor response. PregS, characteristic of more 'bent' steroids, is also typical in its function as an inhibitory neurosteroid[21].

Our lab has shown that both PS and PregS bind to the S1S2 domain of the GluN2B subunit of the NMDA receptor, but that they do not bind to the GluN2D S1S2 domain[22]. Binding of PS and PregS has been found to occur at the ATD of both GluN2B and GluN2D subunits, although the exact binding site is currently unknown.

## III. RESULTS AND DISCUSSION

We hypothesized that neurosteroid binding to the GluN2B and GluN2D subunits occurred at the amino terminal domain. Previous electrophysiology experiments demonstrated that neurosteroids bind to an extracellular region of NMDA receptors, although the exact location of this binding was uncertain. Previous experiments from our lab demonstrated neurosteroid binding to the S1S2 LBD of AMPA receptors. Further fluorescence experiments with NMDA receptors demonstrated that binding of the neurosteroids takes place at the GluN2B S1S2 domain, but not the GluN2D S1S2 domain. This suggests that neurosteroid binding likely occurs at the ATD of both subunits.

The ATDs of GluN2B and GluN2D subunits are about 400 amino acids long. A BLAST homology search was used to determine possible structural domains of these ATDs. With homology to a portion of the atrial natriuretic peptide clearance (ANP-C) receptor precursor, amino acids 121-292 were chosen for cloning and over-expression.

To elucidate neurosteroid binding to the GluN2B and 2D ATDs, intrinsic fluorescence studies were conducted to observe changes in fluorescence emission upon addition of the neurosteroids to each ATD. Intrinsic fluorescence studies measure the changes in emission of intrinsic fluors present in proteins, the amino acids tyrosine, phenylalanine, and tryptophan. However, tyrosine's fluorescence emission is easily quenched and phenylalanine is known to fluoresce weakly. Therefore, the amino acid tryptphan was the amino acid whose emission was measured for fluorescence studies.

There are four tryptophans in this short GluN2B ATD, and three tryptophans in the short GluN2D ATD.

With confirmation of the hypothesis that neurosteroid binding does occur at the GluN2B and 2D ATDs came information that neurosteroid binding is pH dependent, with binding lost after pH 6.5. It was therefore hypothesized that a specific amino acid residue, histidine, played a critical role in neurosteroid binding. Mutations to alter histidine residues were conducted and fluorescence studies were done in order to determine if neurosteroid binding was altered.

**A. Cloning, Growth, & Purification of Wild Type Domains**

GluN2B and GluN2D ATDs were solubly expressed similarly to the S1S2 domains from GluN2D subunits[23]. Soluble protein over-expression proved possible after transformation into Origami 2(DE3) cells.

Circular dichroism (CD) spectroscopy was conducted on wild type (wt) GluN2B and GluN2D ATDS, both apo and bound to the neurosteroids PS and PregS to confirm the presence of secondary structure (Fig. 5A,B). The crystal structure of the GluN2B ATD is known (GluN2D has not yet been crystallized), and has been demonstrated to be a mixture of α-helices and β-sheets (Fig. 5C). Far-UV CD spectroscopy confirmed the purified GluN2D ATD to be folded and of mixed α-helical/β-sheet character, consistent with known structures of the GluN2B ATDs (60% sequence similarity)[24] (pdb id 3JPW (Fig. 5C)).

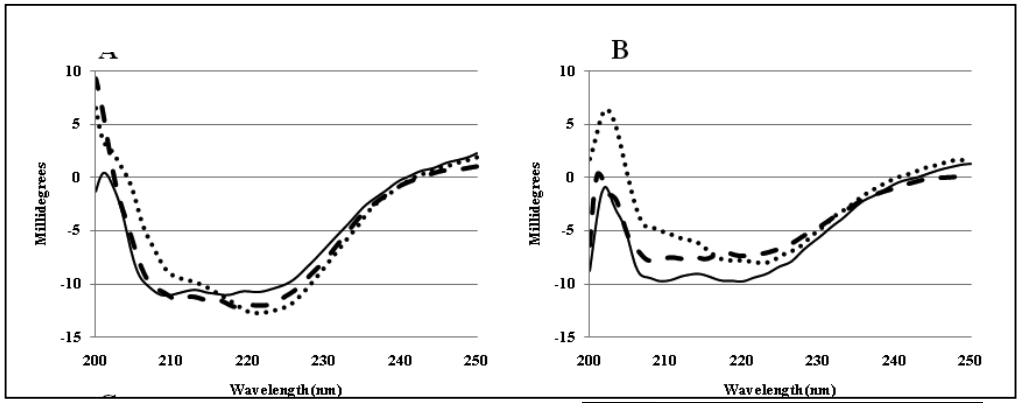


*Fig. 5:* CD spectra of wt GluN2B ATD (5A) and GluN2D ATD (5B) Conc. = 1.7 μM, Apo (- - -), with the addition of 30 fold molar excess of PS (•••) or PREGAS ( ___ ).

(5C) pdb structure of GluN2B ATD-GluN2D ATD crystal structure not determined. Residues 121-292 in blue, His127 in green, residues 4-120 and 293-404 in white.

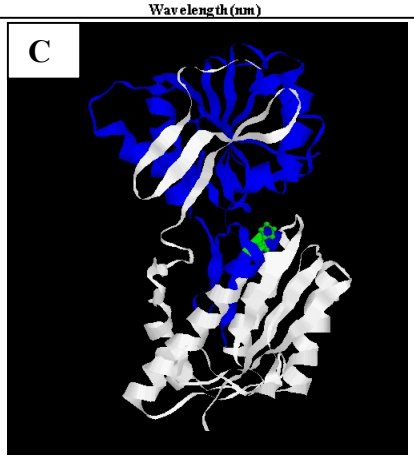


**B. Neurosteroids bind to GluN2B and GluN2D ATDs**

Intrinsic fluorescence studies demonstrated that both neurosteroids, PS and PregS, bind to the GluN2B and GluN2D ATDs (Fig. 6A,B). Binding studies allowed for the determination of the dissociation constant, $K_d$. Calculated $K_d$ values indicate that both PS and PregS bind weakly to the GluN2B and 2D ATDs (Fig. 6A,B). PS demonstrated similar affinity for GluN2B and 2D ATDs. PregS showed a weaker binding affinity than

PS for both ATDs, 2-fold less for the GluN2B ATD, and nearly 6-fold less for the GluN2D ATD.

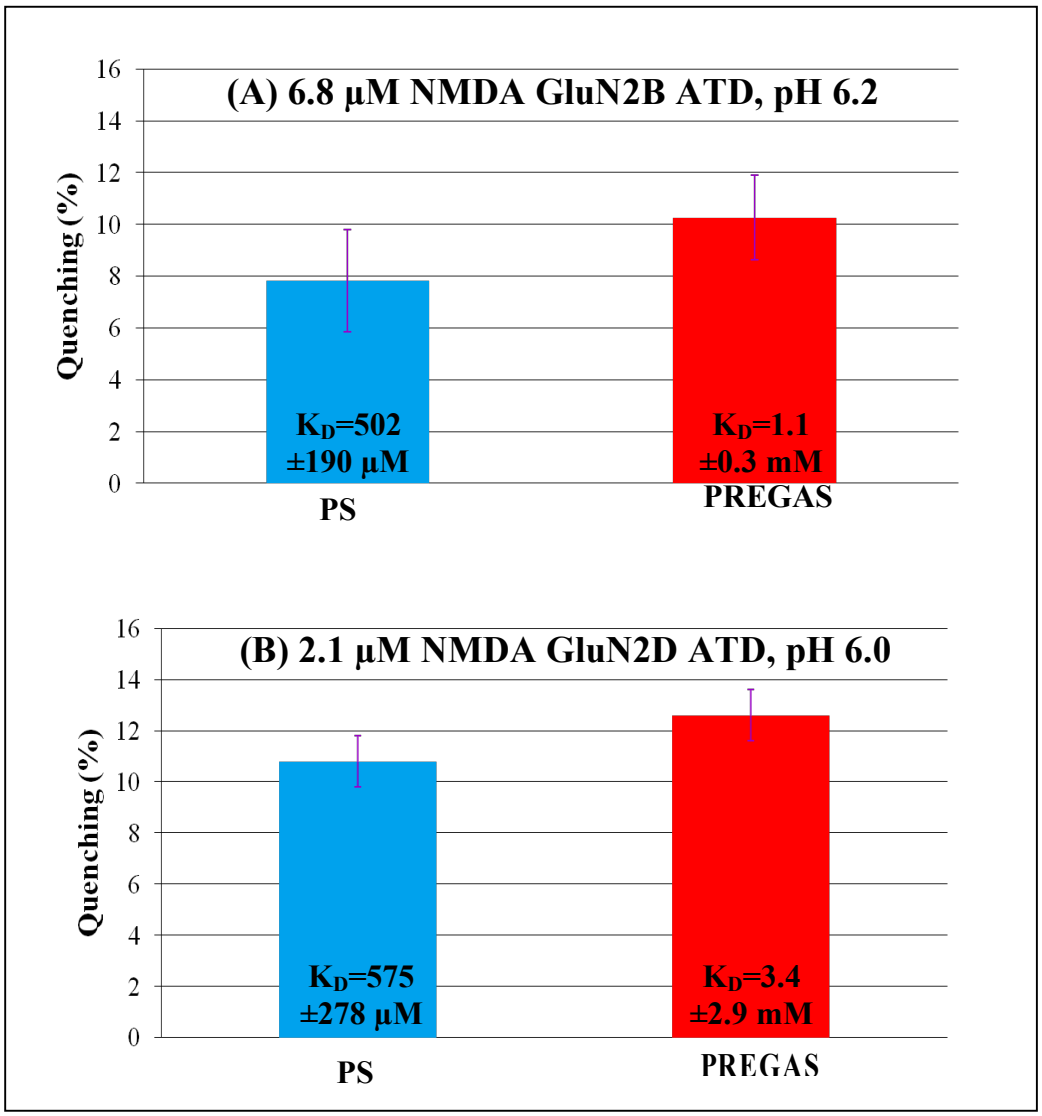


*Fig. 6:* Percent fluorescent quenching of PS and PregS to the GluN2B (A) and GluN2D (B) ATD.

## C. Neurosteroid Binding to Wild Type ATD in pH Dependent Manner

In fluorescence binding studies with the endogenous neurosteroids PS and PregS, it was found that both neurosteroids bound to the GluN2B and GluN2D ATDs, but only at certain pH values (Table 1).

| | pH 6.0 | pH 6.5 | pH 7.0 | pH 7.5 | pH 8.0 |
|---|---|---|---|---|---|
| **GluN2B/2D ATD with PS** | Y | Y | | | |
| **GluN2B ATD with PREGAS** | Y | Y | | | Y |
| **GluN2D ATD with PregS** | Y | Y | Y | | Y |

*Table 1:* pH values at which (30-fold molar excess) neurosteroid binding occurs to 6.8 μM GluN2B and 2.1 μM 2D ATDs, from intrinsic fluorescence studies. "Y" indicates that binding occurs, demonstrated by a change in fluorescence intensity.

Binding of PS and PregS to the ATD was found to occur at the lower pH values of 6.0 and 6.5, and was then lost at higher pH values. Binding was restored for PregS at the higher pH of 8.0, while PS was still unable to bind to the ATDs at that pH value. The loss of binding after pH 6.5 coincides with the ionization of the amino acid histidine, around 6.10. Histidine remains protonated at pH values lower than its pKa, but at pH values of 7 or higher, increasingly large proportions of histidine become neutral. It was hypothesized that histidine, with its ability to both hydrogen bond and/or ionic bond, played a crucial role in neurosteroid binding to the ATD. It was therefore decided to create two mutations for each histidine residue present in the amino terminal domain, the first to glutamine, which is capable of hydrogen but not ionic bonding, and the second to alanine, capable of neither hydrogen nor ionic bonding. By studying whether these two mutants are capable of binding to neurosteroids, more can be determined about the exact location of binding, as well as the type of binding that neurosteroids rely on to bind to the ATD. Using the

crystal structure of the GluN2B ATD (Fig. 5C), the histidine residues for both GluN2B and GluN2D ATDs were mapped.

The work completed thus far focuses on the GluN2D ATD mutants H143A, H182A, H202A, and H202Q. The remaining GluN2D ATD mutants, H143Q and H182Q, are currently being purified. In addition, the GluN2B wild-type ATD, as well as the H127A and H127Q 2B mutants, are in the process of purification.

## D. Mutagenesis, Growth & Purification of GluN2D ATD mutants

The ATD of GluN2B has only 1 histidine (amino acid (aa) 127), which will help locate the binding pocket. The ATD of GluN2D, however, has 3 histidines, aa 143, 182, and 202, which makes identification of the binding pocket more challenging than for the NR2B. Mutagenesis of these four histidines was conducted, changing each histidine to alanine and glutamine. GluN2B and 2D mutant ATDs were solubly expressed according to the protocols established for wild-type amino terminal domains. CD studies were also conducted on two GluN2D mutants, histidine 143 to alanine (H143A) and histidine 202 to glutamine (H202Q) to confirm that the mutation did not result in the loss of secondary structure (Fig. 7).

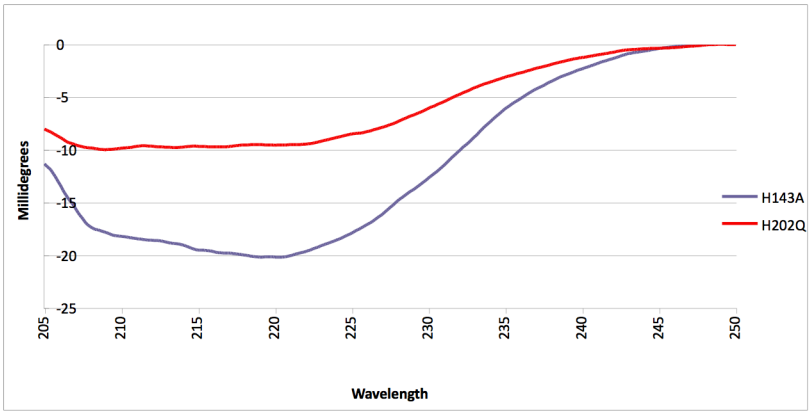


*Fig. 7:* CD spectra of H143A (blue) and H202Q (red) GluN2D ATD mutants (apo), 5.2 μM.

Preliminary results showed that the H143A mutant maintained secondary structure similar to that of the wild type GluN2D ATD, although the CD spectrum was much weaker for the H202Q mutant than the H143A mutant (Fig. 7). Although only one glutamine mutant was investigated, it seems that changing the histidine at 202 to glutamine causes a significant degree of unfolding. This indicates that it is possible aa 202 is crucial for proper folding. Work is currently underway to measure CD spectra for all mutants and compare to the wild type protein under the same conditions.

**E. Fluorescence Studies of GluN2D ATD WT and His Mutants**

Upon determining that wild type and mutant ATDs had secondary structure, intrinsic fluorescence spectroscopy was conducted to determine if there was neurosteroid binding to each ATD at five pH values- 6.0, 6.5, 7.0, 7.5, and 8.0 (Table 2, 3). For the wild type protein there was not enough to conduct fluorescence at all pH values, so there is no fluorescence data for wt at pH 7.0. This will be performed in the future. Fluorescence of the wild type GluN2D ATD when bound to PS (Table 2) and PregS (Table 3) demonstrated higher quenching of both neurosteroids at the lower pH values of 6.0 and 6.5, indicating greater binding.

Intrinsic fluorescence spectroscopy was conducted on four mutant GluN2D ATDs- H143A, H182A, H202A, and H202Q at all five pH values. Upon binding of PS to the three alanine mutations, there appears to be no significant deviation from the wild type binding at the corresponding pH values (Table 2). Thus, although the histidine was mutated, and therefore the ability of the ATD at that particular residue to hydrogen bond

and/or ionic bond was eliminated, neurosteroid binding can still occur. This indicates that either the histidine residues are not important for neurosteroid binding, individually or at all, or perhaps that there are other residues nearby with similar pKas (such as glutamate or cysteine in unique environments) that are affecting the ability of the neurosteroids to bind. The H202Q mutant shows significantly lower ability to bind to PS at all pH values (Table 2), however these results are complicated by the CD data (Fig. 7), indicating significant unfolding of the mutant.

| **pH** | **GluN2D WT** | **H143A** | **H182A** | **H202A** | **H202Q** |
|---|---|---|---|---|---|
| 6.0 | 24.7 ± 3.9 | 21.5 ± 2.32 | 16.3 ± 2.72 | 28 ± 7.28 | **6.7 ± 2.28** |
| 6.5 | 20.2 ± 2.9 | **9.9 ± 5.13** | 13.6 ± 2.33 | 18.7 ± 2.22 | **3.7 ± 2.84** |
| 7.0 | No studies | 8.9 ± 6.39 | 15.7 ± 0.95 | 19.2 ± 5.18 | 8.4 ± 2.8 |
| 7.5 | 6.8 ± 3.12 | NQ | **15.6 ± 1.43** | **17.8 ± 0.87** | NQ |
| 8.0 | 13.1 ± 2.5 | 15.4 ± 5.4 | 13.6 ± 1.6 | 18.3 ± 4.61 | 7.6 ± 3.6 |

*Table 2*: Intrinsic fluorescence quenching of GluN2D ATDs (5.2 μM) in presence of 30 molar excess PS. Percent quenching is measured as ($F_{apo}$ - $F_{neurosteroid}$ / $F_{apo}$) x 100 with error included. NQ indicates no quenching.

PregS, upon binding to the wild type and mutant ATDs, displayed similar tendencies to PS. All three alanine mutants showed a lack of pH dependence, while the H202Q mutant bound even more poorly to PregS than to PS (Table 3). It is currently hypothesized that this decreased binding occurs because of the weaker secondary structure of the H202Q mutant.

| pH | GLuN2D WT | H143A | H182A | H202A | H202Q |
|---|---|---|---|---|---|
| 6.0 | 29.1 ± 5.57 | 17.4 ± 3.55 | 17.1 ± 4.28 | 26.6 ± 5.11 | **NQ** |
| 6.5 | 19.3 ± 2.02 | 18.7 ± 4.13 | **10.7 ± 2.9** | 21.9 ± 2.12 | **NQ** |
| 7.0 | No studies | 13.0 ± 6.46 | 14.6 ± 2.77 | 21.6 ± 3.75 | **4.9 ± 2.4** |
| 7.5 | 6.9 ± 3.17 | **NQ** | 10.4 ± 2.49 | 12.6 ± 2.26 | **NQ** |
| 8.0 | 12.7 ± 3.17 | **NQ** | 11.5 ± 2.62 | 15 ± 2.67 | **NQ** |

*Table 3*: Intrinsic fluorescence quenching of GluN2D ATDs (5.2 μM) in presence of 30 molar excess PregS. Percent quenching is measured as ($F_{apo}$ - $F_{neurosteroid}$ / $F_{apo}$) x 100 with error included. NQ indicates no quenching.

## F. CONCLUSIONS

After confirming that both neurosteroids bind to the GluN2B and GluN2D ATDs in a pH dependent manner, it was hypothesized that histidine's ability to hydrogen bond or ionic bond is crucial to the binding of these neurosteroids. Based on preliminary results, it appears that the binding of these neurosteroids is more complicated than previously thought. It is possible that a glutamate or cysteine, which have pKas similar to histidine in unique environments, could also affect neurosteroid binding. Understanding the possible role of these histidines will allow for further elucidation of the neurosteroid binding pocket in the ATD. Knowledge of this binding pocket would allow for differentiation between potentiation and deactivation of the channel upon binding of the neurosteroid to the ATD, which in turn could lead to possible therapeutic targets.

# IV. EXPERIMENTAL METHODS

## A. Cloning

The ATDs for the NMDA GluN2B, GluN2D, and AMPA GluA2 subunits (amino acids 121-292) were amplified using PCR (rat GluA2 cDNA from Mark Mayer). After restriction digestion (NcoI/XhoI for GluA2 and GluN2D and NcoI/BamHI for GluN2B), these inserts were ligated into similarly cut plasmid pET-GQ, (from Eric Gouaux), and transformed into Origami 2(DE3) cells (Novagen). Colonies were screened by PCR and then sequenced.

## B. Mutagenesis

Site-directed mutagenesis was conducted using a QuikChange XL kit (Stratagene), with primers designed according to Table 4. PCR reactions were set up according to Table 5 and run at 95 °C for 2 min, followed by 18 cycles of 95 °C for 1 min, 68 °C for 50 sec, and 68 °C for 15 min, and ending with one cycle of 68 °C for 7 min. 1 μl *Dpn*1 restriction enzyme was then added to each PCR reaction, spun for 1 min, and incubated at 37 °C for 60 min. 4 μl *Dpn1*-treated DNA were then transformed into XL-10 ultracompetent cells (Stratagene). XL-10 plasmid DNA was transformed into DH5-α competent cells, and next transformed into Origami 2 cells. They were then sequenced.

| | |
|---|---|
| GluN2B H127A | 5’-CCCATCCTGGGCATCGCTGGGGGCTCATCTAT-3’ |
| GluN2B H127Q | 5’-CCCATCCTGGGCATCCAAGGGGGCTCA-3’ |
| GluN2D H143A | 5’-GCGGCGCCGCCGGCCACGGCTACGAT-3’ |
| GluN2D H143Q | 5’-GCCGCCTTGCACGGCTACGA-3’ |
| GluN2D H182A | 5’-CAAGAAGGCCCGAGCGCCTGGGCACGC-3’ |
| GluN2D H182Q | 5’-AAGGCCCGTTGGCCTGGGGCACGC-3’ |
| GluN2D H202A | 5’-CAGCGCTCCTCGAGCCTCCCAGCCCACC-3’ |
| GluN2D H202Q | 5’-GCTGGGAGCAACGAGGAGC-3’ |

*Table 4:* Primer sequences

| Mutant: | H202Q, H127Q (Standard) | H143A, H143Q, H182A, H182Q, H202A | H127A |
|---|---|---|---|
| Buffer | 5 µl | 5 µl | 2.5 µl |
| dsDNA template | 10 ng | 60 ng | 10 ng |
| Primer | 125 ng | 125 ng | 31.25 ng |
| dNTP | 1 µl | 1 µl | 1 µl |
| Quiksolution | 3 µl | 5 µl | none |

*Table 5:* PCR reaction conditions for specific mutants

**C. Protein over-expression and purification**

An overnight of GluN2B or GluN2D ATD in Origami 2(DE3) was used to seed 1.5 L LB-kan (37 °C), with growth continued until an $OD_{600}$ of 0.8 was reached. The temperature was then lowered to 20 °C for 30 min followed by induction with 1 mM IPTG. Growth was continued for 16-18 h at 20 °C, after which time the cells were centrifuged for 10 min at 4 °C and 4,000 rpm. The cell pellets were resuspended in 50 mL buffer A (50 mM Tris, pH 8) containing 5 mM $MgSO_4$, 0.5 mM PMSF, 0.3 mM deoxycholic acid, and 16 μM lysozyme, and lysed by sonication. Lysed cells were centrifuged at 12,500 rpm for 30 min at 4 °C, and the supernatant loaded onto a nickel affinity column (~20 mL, Novagen) and rotated overnight at 4 °C. The column was rinsed with 30 mL of 50, 100, 250, and 500 mM, and 1M imidazole in buffer A. Further purification for the GluN2B or GluN2D ATD included anion exchange chromatography (AEC, GE Q sepharose) at both pH 7.0 and 8.0 (buffer A) followed by size exclusion chromatography (SEC, Superdex 75 10/300) at pH 6.0. The purity of each was determined by SDS-PAGE.

**D. Fluorescence**

Intrinsic fluorescence spectroscopy was performed on a Cary Eclipse fluorometer at 25 °C. All emission scans were acquired from 295-380 nm upon excitation at 280 nm. Final protein concentrations are as specified in figures (GluN2D ATDs in buffer A). The neurosteroids (Steraloids) were solubilized in methanol to 15 mM. A 30:1 molar ratio of neurosteroids was added to each iGluR domain. For all fluorescence experiments: (i)

before data acquisition, samples were incubated for thirty seconds in the sample holder; (ii) to account for any effects methanol had on fluorescence intensity, protein spectra with methanol were collected, allowing for direct comparison; (iii) each data set consisted of three independent spectra of identically prepared samples. For the GluN2B and 2D wild type studies, $K_d$ values were determined by experiments with varying neurosteroid concentration from 25-175 molar excess. A double reciprocal plot [$1/\Delta F = 1/((F_\infty - F_o).K_d[L]) + 1/(F_\infty - F_o)]$, was used to determine $K_d$[25].

**E. Circular Dichroism Spectroscopy**

CD was performed using a JASCO spectrophotometer. 5.2 μM apo protein was added for the GluN2D mutant studies. 1.7 μM GluN2B ATD was used for the wild-type CD, with the addition of 30-fold molar excess of PS and PregS. The GluN2D ATD for the wild-type CD studies was 1.8 μM, again with 30-fold molar excess of PS and PregS. Data was collected from 205-250 nm, 5 times using binomial smoothing (Fig. 5A,B) and 15 times using means-movement smoothing ( Fig. 7). The spectrophotometer operated at room temperature.

## V. FUTURE WORK

The most pressing work to be completed is the growth, purification, and successful completion of ligand binding studies as well as CD studies on the remaining GluN2D mutants (H182Q and H143Q) as well as GluN2B mutants (H127A and H127Q) and the GluN2B wild type ATD. In addition to this, CD thermal denaturation studies will be conducted to determine the relative stability of each mutant's structure as compared to the wild type ATD. $K_D$ studies are also planned, in order to elucidate the binding affinity of neurosteroids for the mutant and wild type ATDs. Upon the completion of these studies, double and triple mutants will also be explored, to elucidate if more than one histidine residue at a time is important for neurosteroid binding, or if glutamate or cysteine play a role.

# VI. REFERENCES


[1] Stern-Bach Y, Bettler B, Hartley M, Sheppard P O, O'Hara P J, Heinemann S F. "Agonist selectivity of glutamate receptors is specified by two domains structurally related to bacterial amino acid-binding proteins."*Neuron.*1994;13: 1345–1357.

[2] Cull-Candy S., Brickley,S. and Farrant,M. (2001) "NMDA receptor subunits: diversity, development and disease." *Curr. Opin. Neurobiol.*, 11, 327–335.

[3] M. Korinek, V. Kapras, V. Vyklicky, E. Adamusova, J. Borovska, K. Vales, A. Stuchlik, M. Horak, H. Chodounska, L. Vyklicky Jr. "Neurosteroid modulation of *N*-methyl-D-aspartate receptors: molecular mechanism and behavioral effects." Steroids, 76 (2011), pp. 1409–1418.

[4] Nusser, Z. "AMPA and NMDA receptors: similarities and differences in their synaptic distribution." *Curr Op Neurobio* 2000, 10: 337-341.

[5] T. Schuler, I. Mesic, C. Madry, I. Bartholomaus, B. Laube. "Formation of NR1/NR2 and NR1/NR3 heterodimers constitutes the initial step in N-methyl-D-aspartate receptor assembly."J Biol Chem, 283 (2008), pp. 37–46.

[6] C.P. Ptak, A.H. Ahmed, R.E. Oswald, "Probing the allosteric modulator binding site of GluR2 with thiazide derivatives." Biochemistry, 48 (2009), pp. 8594–8602.

[7] Armstrong N, Gouaux E. Mechanisms for activation and antagonism of an AMPA-sensitive glutamate receptor: crystal structures of the GluR2 ligand binding core. *Neuron.* 2000;28:165–181.

[8] A.Y. Lau, B. Roux, "The free energy landscapes governing conformational changes in a glutamate receptor ligand-binding domain." Structure, 15 (2007), pp. 1203–1214.

[9] R. Vijayan, M.A. Sahai, T. Czajkowski, P.C. Biggin, "A comparative analysis of the role of water in the binding pockets of ionotropic glutamate receptors." Phys Chem Chem Phys (2010).

[10] Sobolevsky Al, Rosconi MP, Gouaux E: "X-ray structure, symmetry and mechanism of an AMPA-subtype glutamate receptor." *Nature* 2009, 462:745-756.

[11] Mayer, M: "Structure and mechanism of glutamate receptor ion channel assembly, activation and modulation." *Curr Op Neurobio* 2011, 21:283-290.

[12] Shanks NF, Maruo T, Farina AN, Ellisman MH, Nakagawa T: "Contribution of the global subunit structure and stargazing on the maturation of AMPA receptors." *J Neurosci* 2010, 30: 2728-2740.

[13] M. Park-Chung, A. Malayev, R.H. Purdy, T.T. Gibbs, D.H. Farb, "Sulfated and unsulfated steroids modulate gamma-aminobutyric acid A receptor function through distinct sites." Brain Res, 830 (1999), pp. 72–87.

[14] Traynelis S, Wollmuth L, McBain C, et al. Glutamate receptor ion channels: structure, regulation, function. Pharmacol Rev 2010;62:405-496.

[15] M. Park-Chung, F.S. Wu, D.H. Farb, "3 alpha-Hydroxy-5 beta-pregnan-20-one sulfate: a negative modulator of the NMDA-induced current in cultured neurons." Mol Pharmacol, 46 (1994), pp. 146–150

[16] M. Petrovic, M. Sedlacek, M. Horak, H. Chodounska, L. Vyklicky Jr., "20-Oxo-5beta-pregnan-3alpha-yl sulfate is a use-dependent NMDA receptor inhibitor." J Neurosci, 25 (2005), pp. 8439–8450

[17] Spivak, V.; Lin, A.; Beebe, P.; Stoll, L.; and Gentile, L. "Identification of a Neurosteroid Binding Site Contained within the GluR2-S1S2 Domain," *Lipids*, vol. 39, no. 8, 2004.

[18] Malayev A, Gibbs T, Farb D. Inhibition of NMDA response by PS reveals subtype selective modulation of NMDA receptors by sulfated steroids. Br J Pharmacol 2002; 135:901-909.

[19] M. Horak, K. Vlcek, M. Petrovic, H. Chodounska, L. Vyklicky Jr. "Molecular mechanism of pregnenolone sulfate action at NR1/NR2B receptors," J Neurosci, 24 (2004), pp. 10318–10325.

[20] M. Park-Chung, F.S. Wu, R.H. Purdy, A.A. Malayev, T.T. Gibbs, D.H. Farb, "Distinct sites for inverse modulation of *N*-methyl-D-aspartate receptors by sulfated steroids." Mol Pharmacol, 52 (1997), pp. 1113–1123

[21] C.E. Weaver, M.B. Land, R.H. Purdy, K.G. Richards, T.T. Gibbs, D.H. Farb, "Geometry and charge determine pharmacological effects of steroids on *N*-methyl-D-aspartate receptor-induced Ca(2+) accumulation and cell death." J Pharmacol Exp Ther, 293 (2000), pp. 747–75.

[22] Stoll L, Hall J, Van Buren N, et. al. Differential regulation of iGluRs. Biophysical J 2007;92:1343-1349.

[23] Chen G, Sun Y, Gouaux E. Probing ligand binding domain of GluR2 receptor by proteolysis and deletion mutagenesis defines domain boundaries and yields crystallizable construct. Protein Sci 1998;7:2623-2630.

[24] Karakas E, Simorowski N, Furukawa H. Subunit arrangement and phenylethanolamine binding of GluN1/GluN2B NMDA receptors. Nature 2011;475:249-253.

[25] Raabe R, Gentile L. Antidepressant interactions with NMDA NR1-1b. J Biophysics 2008; Article ID 474205,doi:10.1155/2008/474205.